

# Energy Level Diagrams for Black Hole Orbits

Janna Levin

Department of Physics and Astronomy, Barnard College of Columbia University, 3009 Broadway, New York, NY 10027 and  
Institute for Strings, Cosmology and Astroparticle Physics (ISCAP), Columbia University, New York, NY 10027

janna@astro.columbia.edu

A spinning black hole with a much smaller black hole companion forms a fundamental gravitational system, like a colossal classical analog to an atom. In an appealing if imperfect analogy to atomic physics, this gravitational atom can be understood through a discrete spectrum of periodic orbits. Exploiting a correspondence between the set of periodic orbits and the set of rational numbers, we are able to construct periodic tables of orbits and energy level diagrams of the accessible states around black holes. We also present a closed form expression for the rational  $q$ , thereby quantifying zoom-whirl behavior in terms of spin, energy, and angular momentum. The black hole atom is not just a theoretical construct, but corresponds to extant astrophysical systems detectable by future gravitational wave observatories.

Bare black holes are as perfect as fundamental particles. As Chandrasekhar said, “The black holes of nature are the most perfect macroscopic objects there are in the universe [1]”. A black hole with a given mass and spin is indistinguishable from every other black hole with the same mass and spin. Likewise, a supermassive black hole with a much smaller black hole companion forms a kind of macroscopic, classical atom, reminiscent of the hydrogen atom. In analogy with atomic physics, the orbits around a given black hole can be completely described by a periodic table [2] – a table of periodic orbits ordered in ascending energy from the stable circular orbits (the ground-like state) up to the last bound orbits (the energy of ionization). Further, the energy levels of the periodic orbits around a black hole are, formally speaking, discrete. In the spirit of this atomic analogy [? ], we exploit energy level diagrams as another valuable representation of the dynamics around a black hole nucleus.

The energy level diagrams are based on an infinite ordered set of periodic orbits around a Kerr black hole [2]. Fig. 1 shows a periodic table of retrograde orbits. At first glance, the set of idealized, closed orbits might seem improbably special. Yet the periodic set is fundamental to an understanding of the entire dynamics. As we now elaborate, *all* orbits are near a periodic orbit, and therefore this seemingly special set is able to encode the entire orbital dynamics.

## I. PERIODIC ORBITS AND THE RATIONAL NUMBERS

Our atomic analogy will stem from a mapping between black hole orbits and rational numbers. For the sake of argument, we consider orbits confined to the equatorial plane. Any equatorial orbit around a black hole has two

fundamental frequencies<sup>1</sup> – the libration in the radial coordinate,  $\omega_r$ , and the rotation in the angular coordinate,  $\omega_\varphi$ . To be clear, by  $\omega_r$  we mean the frequency of radial oscillations,  $\omega_r = 2\pi/T_r$ , where  $T_r$  is the time it takes to move from one apastron to another. By  $\omega_\varphi$ , we mean the average angular frequency over a radial oscillation,  $\omega_\varphi = T_r^{-1} \int_0^{T_r} (d\varphi/dt) dt$ . A generic orbit will have frequencies that are irrationally related and will consequently never close. Instead, it precesses around the central black hole nucleus, never returning exactly to its starting point. In contrast, a special set of orbits – the periodic orbits – will close. For this to be the case, the two fundamental frequencies must be commensurate, that is, rationally related. We define the rational number  $q$  associated with each periodic orbit through

$$\frac{\omega_\varphi}{\omega_r} = 1 + q \quad . \quad (1)$$

Since the set of irrationals is a larger infinity than the set of rationals, the rationals are a set of measure zero in the space of all possible orbits.

However, the set of periodic orbits are dense on the number line. Any irrational can be arbitrarily well approximated by a nearby rational. A good way to find the rational approximant is to use continued fractional expansions. Let  $\sigma$  be some irrational number and let  $1 + \sigma$  be the irrational ratio of frequencies for some generic orbit. Such a trajectory precesses around the central black hole without ever closing. The irrational can be represented through continued fractions as

$$\sigma = w + \frac{1}{a_1 + \frac{1}{a_2 + \frac{1}{a_3 + \dots}}} \quad (2)$$

where  $w$  is the integer part of  $\sigma$ ,  $a_1$  is the integer part of the reciprocal of  $\sigma - w$ ,  $a_2$  is the integer part of the

---

<sup>1</sup> Non-equatorial orbits have three fundamental frequencies and therefore are designated by two rationals.

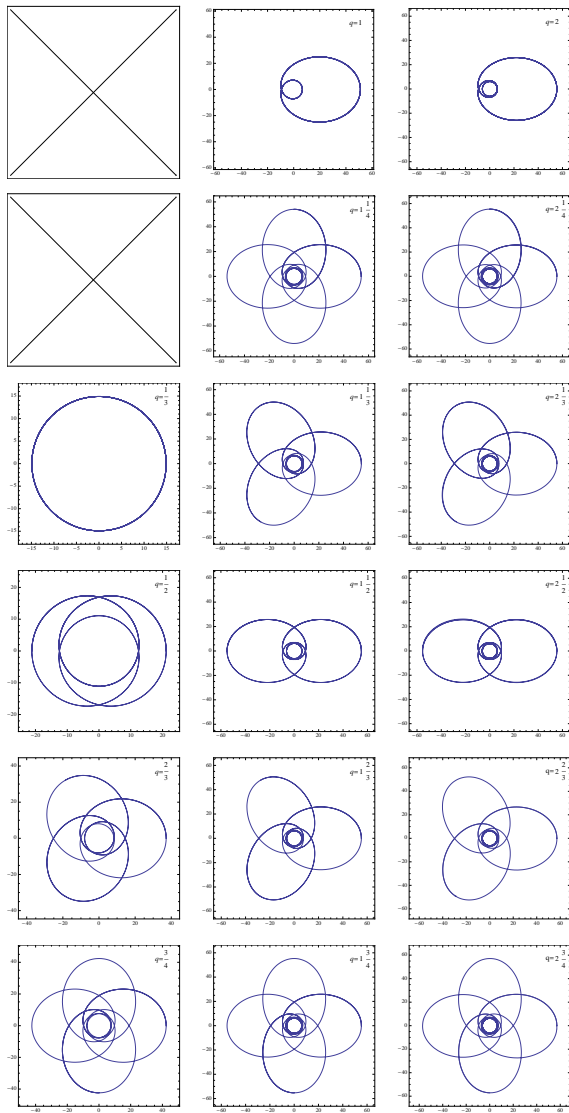


FIG. 1: A periodic table for retrograde equatorial orbits around a black hole with spin parameter  $a = -0.9$ . The angular momentum is  $L = 4.56056$ . All entries with  $z \leq 4$  and  $0 \leq w \leq 2$  are included. Energy increases from top to bottom and then left to right, as does the rational  $q = w + v/z$ . The columns are  $w$ -bands 0, 1, 2 from left to right. The minimum is  $q \neq 0$ , as discussed in §III and §IV. Although we have drawn 3 columns, there are in principle an infinite number as  $w \rightarrow \infty$ .

reciprocal of the remainder of  $a_1$  etc. through an infinite list of integers  $a_n$ . A given rational approximant is obtained by truncating the continued fraction at some finite  $n$ . For instance, if we truncate the continued fractional expansion at  $n = 3$ , then

$$\sigma \approx q = w + \frac{v}{z} = w + \frac{a_2 a_3 + 1}{a_1 a_2 a_3 + a_1 + a_3}. \quad (3)$$

In this way, any irrational can be arbitrarily well approximated by rationals; significantly then, any aperiodic orbit (with an irrational frequency ratio) can be arbitrarily

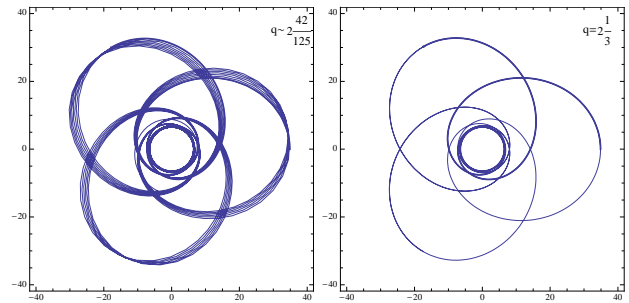


FIG. 2: Left: A generic retrograde orbit around a central black hole with spin parameter  $a = -0.995$ . The angular momentum  $L$  is halfway between the ibco (innermost bound circular orbit) and the isco (innermost stable circular orbit). This orbit has an energy very near the 3-leaf orbit on the right.

well approximated by some periodic orbit (with a rational frequency ratio).

To illustrate, the generic aperiodic orbit on the left of Fig. 2, if allowed to run indefinitely, would fill an annulus in the plane, never closing. This is a generic example of zoom-whirl behavior. (For other discussions of zoom-whirl behavior see [3].) Yet this same orbit has a  $\sigma \approx q = 2 + 42/125$ , and so is very close to a periodic orbit that whirls 2 times, has 125 leaves but skips to the 42nd next leaf in the pattern each successive time it hits apastron. Also note that the orbit is still close to, but not as well approximated by, the much lower-leaf orbit characterized by the rational  $q = 2 + 1/3$ , drawn on the right of Fig. 2. Indeed, the generic orbit can be thought of as a precession of this fundamental three-leaf pattern by the amount  $2\pi(42/125 - 1/3) = 2\pi/375$  – so less than one degree – each radial cycle. In fact, in general, all high-leaf orbits can be understood as precessions of lower-leaf orbits [2].

For emphasis, every orbit that is measured observationally or generated numerically is necessarily truncated by a rational approximant and is therefore, strictly speaking, periodic, albeit possibly with an extremely long period. Consequently the orbital dynamics around the central black hole is entirely defined by the periodic skeleton. Furthermore, high-leaf periodics can be understood as precessions of lower-leaf periodics.

Although we restrict to two-dimensional equatorial motion here, generic three-dimensional non-equatorial orbits can also be identified with rational numbers. In principle, two rationals are needed to characterize a completely closed non-equatorial orbit, the  $q$  we are using as well as a  $q_\Phi = \omega_\theta/\omega_r$ . However, it should be mentioned that we do not need to require fully closed motion, as shown in Refs. [? ?] in the context of comparable mass binaries. The useful insight is the simple observation that every orbit lies in its own orbital plane, even if it does not lie in the equatorial plane. Periodic tables of *orbital plane* motion were shown to taxonomize orbits with one rational,  $q_\Phi$  where  $\Phi$  is the angle swept out in

the orbital plane, just as the periodic tables of equatorial orbits are taxonomized by the  $q$  above. The entire orbital plane then precesses to trace out fully three-dimensional motion, although not necessarily fully periodic motion. For the rest of this paper, we will restrict to equatorial motion for transparency.

## II. $q$ AND ITS TOPOLOGICAL SIGNIFICANCE

We can relate the triplet of integers  $(z, w, v)$  in the definition of the rational

$$q = w + v/z \quad (4)$$

to geometric and topological features of the orbit. Consider Fig. 1 again. The periodic orbits are assembled in a table of increasing energy – as is the chemical periodic table. In our tables, energy increases from top to bottom and left to right. Note that the  $q$  of the periodic table increases monotonically with energy.

Each  $q$  also has a geometric interpretation. Consider its definition

$$q = w + \frac{v}{z} \equiv \frac{\omega_\varphi}{\omega_r} - 1 = \frac{\Delta\varphi}{2\pi} - 1 \quad (5)$$

where  $\Delta\varphi = \int^{T_r} (d\varphi/dt)dt$  is the equatorial angle accumulated in one radial cycle from apastron to apastron. By this definition, we see that  $q$  is the amount an orbit precesses beyond the closed ellipse. Therefore Kepler's elliptical orbits have  $q = 0$  since there is no precession. Keplerian orbits are all periodic. They are also relativistically excluded. Relativistic orbits around black holes all overshoot their starting point, which is to say they all precess, a discovery that originates with Mercury's famed precession, and all relativistic orbits have a  $q > 0$ .

Note that all of the orbits in the second column of the periodic table of Fig. 1 whirl an additional  $2\pi$  in a nearly circular loop around the nucleus before moving out to the next apastron. The entries in the third column whirl twice. The integer part of  $q$  from equation (5), denoted by  $w$ , is the number of whirls. The periodic tables are ordered in terms of  $w$ -bands, which form energy bands. In fact, unlike the chemical periodic table, the black hole periodic table in Fig. 1 has infinitely many columns, one for each possible integer number of whirls.

Within each energy band, each  $w$ -band, the entries are  $z$ -leaf orbits that whirl  $w$  times between each apastron. Closed orbits can skip leaves each radial period. For example, the third and fifth entries of column 2 in the periodic tables are both 3-leaf clovers but they are not identical. The third entry in column 2 moves to the next apastron in the 3-leaf pattern as indicated in bold. However, the fifth entry in column 2 moves to the second apastron in the 3-leaf pattern as indicated in bold. According to equation (5), the  $q$  of the former closed orbit is  $q = w + v/z = 1 + 1/3$  while the  $q$  of the latter is  $q = w + v/z = 1 + 2/3$ . So  $v$  labels the order in which the leaves are hit.

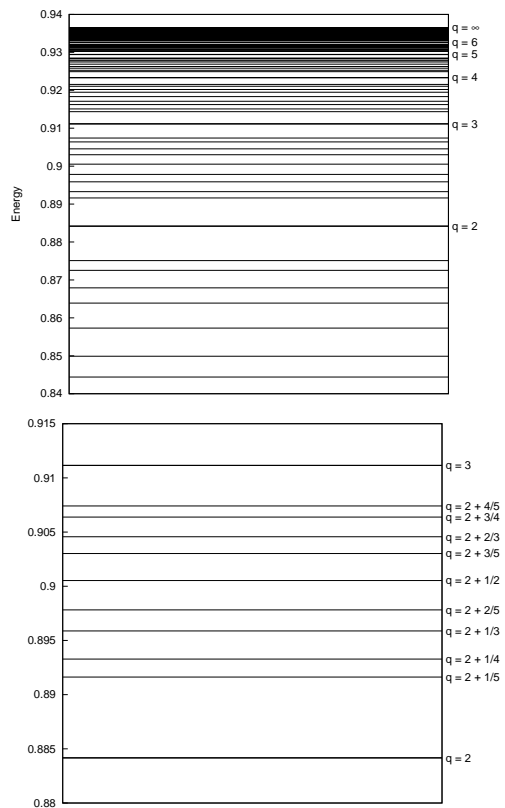


FIG. 3: Energy Level diagrams for equatorial orbits with  $L = 2$  around a central black hole with spin parameter  $a = 0.995$ . All  $z \leq 5$  for all  $1 \leq w \leq 12$  are included although the  $q = 1\frac{1}{5}$  and  $q = 1\frac{1}{4}$  entries are missing from the  $w = 1$  band since they are not accessible. The figure on the bottom shows a detail of the top figure, indicating the rationals within the  $w = 2$  band.

The rational number identifying a given periodic orbit therefore encodes significant topological and geometric information. It identifies the number of leaves, the number of whirls, and the order in which the leaves are traced.

## III. ENERGY LEVEL DIAGRAMS

Since the rationals are discrete, it follows that the energies of the periodic orbits are likewise discrete. Furthermore, as discovered in Ref. [2],  $q$  is monotonic with energy (for a given angular momentum  $L$  around a given black hole). This latter observation allows us to represent the information in a periodic table in a related energy level diagram as shown in Fig. 3.

Energy level diagrams provide a valuable complement to the periodic tables, effectively and concisely summarizing information. For instance, Fig. 3 incorporates all  $z \leq 5$  orbits for  $1 \leq w \leq 12$ , while the corresponding periodic table of Fig. 1 only includes  $z \leq 4$  for  $0 \leq w \leq 2$ .

The energy level diagram illustrates the stacking of

energy levels for all orbits into bulk  $w$ -bands. The fractional part of  $q$ , represented by  $v/z$ , has an intriguing distribution within a given band that roughly repeats in a scaled manner throughout all  $w$ -bands.

If we were to draw every one of the infinite  $q$ 's allowed, they would, despite being discrete, fill a solid wall of color for each  $w$ -band. Still, even though there are always an infinite number of entries in any periodic table, high- $z$  orbits can be approximated as precessions around low- $z$  clovers. In practice, we can restrict to a finite set of discrete rationals.

Furthermore, not all rationals are accessible for a given angular momentum,  $L$ , around a given black hole. The lower limit is set by the  $q$  of the ground state – equivalently, the  $q$  of the stable circular orbit – and the upper limit is set by the  $q$  of the highest-energy bound orbit. Both upper and lower limits depend on  $L$  and the spin of the central black hole.

Although initially counter-intuitive, the lower limit is not simply 0. As in Ref. [2], we take the  $q$  for the ground state, that is, for a given stable circular orbit, to be  $q_c \rightarrow \omega_\varphi/\omega_r - 1$  in the limit of eccentricity going to zero. This minimum  $q$  is not zero. For the energy level diagram of Fig. 3, the bound on  $q$  is roughly  $1 + 1/3 < q < \infty$ . Importantly, this means that some low  $q$  orbits are not accessible in the strong-field regime. Namely, Mercury-type orbits, which as precessions of Keplerian ellipses would correspond to rationals  $0 < q \ll 1$ , are forbidden in the strong-field regime and *all* allowed states will look like precessions of multi-leaf orbits. We will also write down an explicit analytic expression for  $q_c$  in §IV.

As the angular momentum increases both the lower and upper bounds will eventually decrease toward zero, so that, as we know from solar system dynamics, all orbits in the Newtonian approximation are tight precessions of the ellipse.

#### IV. CLOSED FORM EXPRESSION FOR $q(a, E, L)$

We can always numerically integrate the Kerr equations to find  $q$ . However, it is useful to have a closed form expression purely in terms of  $(a, E, L)$ . Such a closed form should be advantageous when considering the evolution of  $q$  under the dissipative effects of gravitational radiation [? ]. Starting with the definition

$$q = \frac{2}{2\pi} \int_{r_p}^{r_a} \frac{\dot{\varphi}}{\dot{r}} dr - 1 \quad , \quad (6)$$

we can perform this integral to generate an expression in terms of elliptical integrals. We will take the further step of finding the limits of integration in terms of  $(a, E, L)$  so that our final expression will automatically deliver  $q$  given  $(a, E, L)$  as the only input.

We rewrite [2] the geodesic equations for Kerr equatorial orbits [4] as

$$\begin{aligned} r^2 \dot{r} &= \pm \sqrt{R} \\ r^2 \dot{\varphi} &= -\frac{1}{\Delta} \frac{\partial R}{\partial L} \end{aligned} \quad (7)$$

where an overdot denotes differentiation with respect to the particle's proper time  $\tau$  and

$$\begin{aligned} R(r) &= P^2 - \Delta \{r^2 + (L - aE)^2\} \\ P(r) &= E(r^2 + a^2) - aL \\ \Delta &\equiv r^2 - 2r + a^2 \quad , \end{aligned} \quad (8)$$

where the mass of the black hole is set to  $M = 1$ .

We then have

$$q = \frac{1}{\pi} \int_{r_p}^{r_a} \left( \frac{-(aE - L) + \frac{a}{\Delta} P}{\sqrt{R}} \right) dr - 1 \quad , \quad (9)$$

where we take the plus sign in  $\dot{r}$  indicating we are integrating from periastron,  $r_p$ , out to apastron,  $r_a$ .

To solve this, we write both  $R$  and  $\Delta$  in terms of their roots.  $R$  is a fourth-order equation in  $r$ . In the equatorial plane, one of the roots is always 0 and  $R$  can be written

$$R(r) = (E^2 - 1)r(r - r_0)(r - r_p)(r - r_a) \quad (10)$$

while we can write  $\Delta$  in terms of the inner and outer horizons  $r_\pm = 1 \pm \sqrt{1 - a^2}$ :

$$\Delta = (r - r_+)(r - r_-) \quad . \quad (11)$$

We want to solve

$$\begin{aligned} q &= -\frac{1}{\pi}(aE - L) \int_{r_p}^{r_a} \frac{dr}{\sqrt{R}} + \frac{1}{\pi}a^2(aE - L) \int_{r_p}^{r_a} \frac{dr}{\Delta\sqrt{R}} \\ &\quad + \frac{1}{\pi}aE \int_{r_p}^{r_a} \frac{r^2 dr}{\Delta\sqrt{R}} - 1 \quad , \end{aligned} \quad (12)$$

which we rewrite as

$$\begin{aligned} q &= \left[ -\frac{1}{\pi}(aE - L)\mathcal{I}_1 + \frac{1}{\pi}a^2(aE - L)\mathcal{I}_2 + \frac{1}{\pi}aE\mathcal{I}_3 \right]_{r_p}^{r_a} - 1 \\ \mathcal{I}_1 &= \int \frac{dr}{\sqrt{R}} \\ \mathcal{I}_2 &= \int \frac{dr}{\Delta\sqrt{R}} \\ \mathcal{I}_3 &= \int \frac{r^2 dr}{\Delta\sqrt{R}} \quad . \end{aligned} \quad (13)$$

Defining

$$\begin{aligned} \alpha(r) &= \frac{r(r_p - r_0)}{r_p(r - r_0)} \\ \beta(r) &= \frac{r(r_p - r_a)}{r_p(r - r_a)} \\ \gamma(r) &= \frac{(r - r_0)(r_a - r_p)}{(r_a - r_0)(r - r_p)} \end{aligned} \quad (14)$$

the solutions are

$$\begin{aligned}\mathcal{I}_1(r) &= \frac{2}{\sqrt{(E^2-1)r_p(r_0-r_a)}} \text{EllipticF} \left[ \text{ArcSin} \left[ \frac{1}{\sqrt{\gamma(r)}} \right], \beta(r_0) \right] \\ \mathcal{I}_1(r_a) &= \frac{2}{\sqrt{(E^2-1)r_p(r_0-r_a)}} \text{EllipticK} [\beta(r_0)]\end{aligned}\quad (15)$$

with  $\mathcal{I}_1(r_p) = 0$ ; The second integral is

$$\begin{aligned}\mathcal{I}_2 &= \frac{-2}{a^2 \sqrt{(E^2-1)r_p(r_a-r_0)}} \left( \text{EllipticF} \left[ \text{ArcSin} \left[ \alpha(r)^{-1/2} \right], \alpha(r_a) \right] \right. \\ &\quad + \frac{r_0 r_+}{(r_0-r_-)(r_- - r_+)} \text{EllipticPi} \left[ \alpha(r_-), \text{ArcSin} \left[ \alpha(r)^{-1/2} \right], \alpha(r_a) \right] \\ &\quad \left. + \frac{r_0 r_-}{(r_0-r_+)(r_+ - r_-)} \text{EllipticPi} \left[ \alpha(r_+), \text{ArcSin} \left[ \alpha(r)^{-1/2} \right], \alpha(r_a) \right] \right)\end{aligned}$$

This gives non-zero contributions at both limits of integration; Finally, we have

$$\begin{aligned}\mathcal{I}_3 &= \frac{2(r_p-r_0)}{\sqrt{(E^2-1)r_p(r_0-r_a)}} \\ &\quad \left( \frac{r_0^2}{(r_0-r_-)(r_p-r_0)(r_0-r_+)} \text{EllipticF} \left[ \text{ArcSin} \left[ \frac{1}{\sqrt{\gamma(r)}} \right], \beta(r_0) \right] \right. \\ &\quad + \frac{r_-^2}{(r_0-r_-)(r_- - r_p)(r_- - r_+)} \text{EllipticPi} \left[ \gamma(r_-), \text{ArcSin} \left[ \frac{1}{\sqrt{\gamma(r)}} \right], \beta(r_0) \right] + \\ &\quad \left. \frac{r_+^2}{(r_0-r_+)(r_+ - r_p)(r_+ - r_-)} \text{EllipticPi} \left[ \gamma(r_+), \text{ArcSin} \left[ \frac{1}{\sqrt{\gamma(r)}} \right], \beta(r_0) \right] \right)\end{aligned}\quad (16)$$

At  $r = r_a$ ,  $\gamma(r_a) = 1$  and an EllipticF becomes an EllipticK, while at  $r = r_p$ ,  $\gamma(r_p) = \infty$  and EllipticF and EllipticPi become zero. So evaluating this at the upper and lower limits gives

$$\begin{aligned}\mathcal{I}_3(r_a) &= \frac{2(r_p-r_0)}{\sqrt{(E^2-1)r_p(r_0-r_a)}} \\ &\quad \left( \frac{r_0^2}{(r_0-r_-)(r_p-r_0)(r_0-r_+)} \text{EllipticK} [\beta(r_0)] \right. \\ &\quad + \frac{r_-^2}{(r_0-r_-)(r_- - r_p)(r_- - r_+)} \text{EllipticPi} [\gamma(r_-), \beta(r_0)] + \\ &\quad \left. \frac{r_+^2}{(r_0-r_+)(r_+ - r_p)(r_+ - r_-)} \text{EllipticPi} [\gamma(r_+), \beta(r_0)] \right) .\end{aligned}\quad (17)$$

We use these to evaluate

$$q = -\frac{1}{\pi}(aE-L)\mathcal{I}_1(r_a) + \frac{1}{\pi}a^2(aE-L)[\mathcal{I}_2(r_a) - \mathcal{I}_2(r_p)] + \frac{1}{\pi}aE\mathcal{I}_3(r_a) - 1 \quad (18)$$

We are not quite done since this expresses  $q(a, E, L, r_0, r_p, r_a)$ . To have  $q$  as a function of  $(a, E, L)$  only, we have to find  $r_0, r_p, r_a$  as functions of  $(a, E, L)$ . To do so we expand the polynomial  $R(r) = (E^2-1)r(r-r_0)(r-r_p)(r-r_a)$  and equate to the definition of  $R(r)$  in Eq. (8), matching up coefficients in powers of  $r$  and finding a system of equations for  $r_0, r_p, r_a$ . Since  $r = 0$  is always a root, this is equivalent to a 3rd order equation in  $r$  and cubic equations have a generic solution. We want the roots of

$$\begin{aligned}R(r) &= 0 \\ Ar^3 + Br^2 + Cr + D &= 0 \\ A &= (E^2-1) \\ B &= 2 \\ C &= Aa^2 - L^2 \\ D &= 2(L - aE)^2\end{aligned}\quad (19)$$

The nonzero roots in ascending order are

$$\begin{aligned} r_0 &= -\frac{B}{3A} - \frac{2^{1/3}(-B^2 + 3AC)}{3A}(F + \sqrt{G})^{-1/3} + \frac{1}{3A2^{1/3}}(F + \sqrt{G})^{1/3} \\ r_p &= -\frac{B}{3A} + \frac{(1 - i\sqrt{3})(-B^2 + 3AC)}{3A2^{2/3}}(F + \sqrt{G})^{-1/3} - \frac{1 + i\sqrt{3}}{6A2^{1/3}}(F + \sqrt{G})^{1/3} \\ r_a &= -\frac{B}{3A} + \frac{(1 + i\sqrt{3})(-B^2 + 3AC)}{3A2^{2/3}}(F + \sqrt{G})^{-1/3} - \frac{1 - i\sqrt{3}}{6A2^{1/3}}(F + \sqrt{G})^{1/3} \end{aligned} \quad (20)$$

where

$$\begin{aligned} F &= -2B^3 + 9ABC - 27A^2D \\ G &= F^2 - 4(B^2 - 3AC)^3 \end{aligned} \quad (21)$$

Using Eqs. (20) in Eq. (18), gives the rational  $q$  as a function of  $(a, E, L)$ , which is what we were after.

To be clear, the function  $q(a, E, L)$  of Eq. (18) can in principle be any positive real number. The periodic orbits correspond to rational  $q$ . All other orbits can be arbitrarily well approximated by a rational  $q$  as discussed previously. As a check, inputting the  $(a, E, L)$  of the retrograde orbit on the right of Fig. 2 returns a  $q = 2.3333\dots = 2\frac{1}{3}$ , as it should.

While Eq. (18) gives the  $q$  for a generic equatorial orbit, it is interesting to write out the expression for the lower limit of stable circular orbits explicitly. Circular orbits have a radius  $r_c = r_a = r_p$  and this leads to a great simplification in the expression since then  $\beta(r_0) = \gamma(r_+) = \gamma(r_-) = 0$  and  $\text{EllipticK}[0] = \text{EllipticPi}[0, 0] = \pi/2$ . Using these relations gives

$$q_c = \frac{1}{\sqrt{(E^2 - 1)r_c(r_0 - r_c)}} \left[ -(aE - L) + aE \frac{r_c^2}{\Delta(r_c)} \right]$$

The root  $r_0$  corresponding to a given  $r_c$  can be found from the cubic expressions above evaluated at the energy and angular momenta of circular orbits, originally found in Ref. [?] ]

$$E = \pm \frac{r_c^{3/2} - 2r_c^{1/2} \pm a}{r_c^{3/4} \sqrt{r_c^{3/2} - 3r_c^{1/2} \pm 2a}} \quad (22)$$

$$L = \pm \frac{r_c^2 \mp 2ar_c^{1/2} + a^2}{r_c^{3/4} \sqrt{r_c^{3/2} - 3r_c^{1/2} \pm 2a}} \quad , \quad (23)$$

where the  $\pm$  refers to prograde and retrograde orbits respectively.

Alternatively, and perhaps more easily, we can write the roots as functions of  $(a, E, L)$  by expanding,

$$\begin{aligned} R(r)/r &= 0 \\ &= (E^2 - 1)(r - r_0)(r - r_c)^2 \\ &= (E^2 - 1)(r^3 - r^2(r_0 + 2r_c) + r(r_c^2 + 2r_0r_c) - r_0r_c^2) \end{aligned}$$

to find the  $r \neq 0$  roots when  $r_a = r_p$  are degenerate at the value  $r_c$ . Equating coefficients with those of Eq. (19)

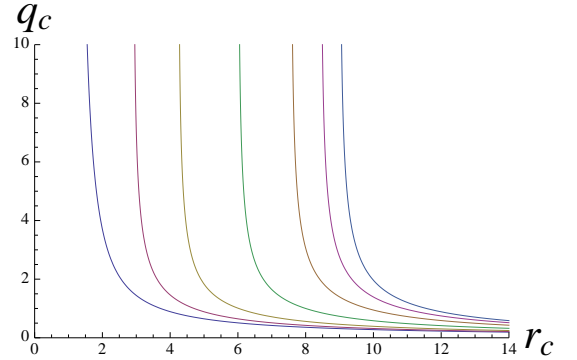


FIG. 4:  $q_c$  for circular orbits for spin values from left to right  $a = 0.998, 0.8, 0.5, 0, -0.5, -0.8, -0.998$ . Negative spin values are equivalent to retrograde orbits. The value of  $q_c$  diverges at the innermost stable circular orbit (ISCO) for each value of the spin as expected [2].

gives

$$\begin{aligned} A &= (E^2 - 1) \\ -A(r_0 + 2r_c) &= 2 \\ A(r_c^2 + 2r_0r_c) &= Aa^2 - L^2 \\ -Ar_0r_c^2 &= 2(L - aE)^2 \end{aligned} \quad , \quad (24)$$

and

$$\begin{aligned} r_c &= -\frac{2}{3(E^2 - 1)} \left[ 1 + \sqrt{1 - \frac{3(E^2 - 1)}{4} ((E^2 - 1)a^2 - L^2)} \right] \\ r_0 &= -\frac{2}{(E^2 - 1)} - 2r_c \end{aligned} \quad (25)$$

When solving the quadratic, the sign consistent with  $(r_c - r_0) > 0$  is chosen. Note that for all bound orbits  $E^2 - 1 < 0$ .



The value of  $q_c$  for different spins is shown in Fig. 4. In the strong-field, the ground state has a  $q_c$  well above zero, ruling out Mercury-type precessions in favor of the more extreme zoom-whirl precessions.

## V. GRAVITATIONAL RADIATION

In addition to being fundamental, the black hole atoms have the added benefit of being real. Black hole pairs formed by tidal capture in dense regions, such as globular clusters [?] or the galactic nucleus [? ?], will likely become bound on eccentric orbits. Light black holes that fall onto supermassive black holes in the galactic nucleus are also free to be eccentric. Supermassive black holes with stellar mass black hole companions are candidates for direct detection through gravitational radiation by LISA (Laser Interferometer Space Antenna). As entries in the periodic tables, we can identify the  $q$  of these black hole inspirals as a function of  $(a, E, L)$  given the results of this paper. This allows us to predict the relativistic zoom-whirl behavior from a simple formula.

In our periodic tables and energy level diagrams we have neglected the dissipative effects of gravitational radiation. As energy and angular momentum are radiated away in the form of gravitational waves, there will be transitions from the orbits of one energy level diagram at a given  $L$  to those of another energy level diagram at lower  $L$ .

The rate of change of  $q$  can be expressed in terms of the change of energy and angular momentum as

$$\frac{dq}{dt} = \frac{\partial q}{\partial E} \frac{dE}{dt} + \frac{\partial q}{\partial L} \frac{dL}{dt} . \quad (26)$$

This can be evaluated by explicitly taking the derivatives of (18), being sure to treat  $r_0, r_p, r_a$  as functions of  $(E, L)$  through Eqs. (20). Accurate calculations of  $dE/dt$  and  $dL/dt$  for zoom-whirl orbits require detailed numerical computations [5, 6, 7]. In conjunction with such computations, our closed form expression for  $q$  would enable us to find possible resonances during inspiral [8], which occur during episodes of  $dq/dt \approx 0$ . As seen in Fig. 5,  $\partial q/\partial E > 0$  and  $\partial q/\partial L < 0$ . Consequently, it is possible that the condition  $\Delta q \approx 0$  will be satisfiable:

$$\frac{\partial q}{\partial E} \Delta E \approx - \frac{\partial q}{\partial L} \Delta L , \quad (27)$$

during inspiral and an orbit will noticeably hang near a given  $q$  for a time. While a detailed study will require a full numerical treatment of adiabatic inspiral, we mention

that in the simulations of Ref. [9], it can be seen by eye that the orbit will occasionally hang on a very nearly closed orbit as it sweeps through to merger.

In full numerical relativity we have seen  $q$  change rapidly for comparable mass black hole pairs [?]. By contrast, an extreme-mass-ratio system can spend hundreds to thousands of orbits in the strong-field regime where periodic tables are most illuminating. The small

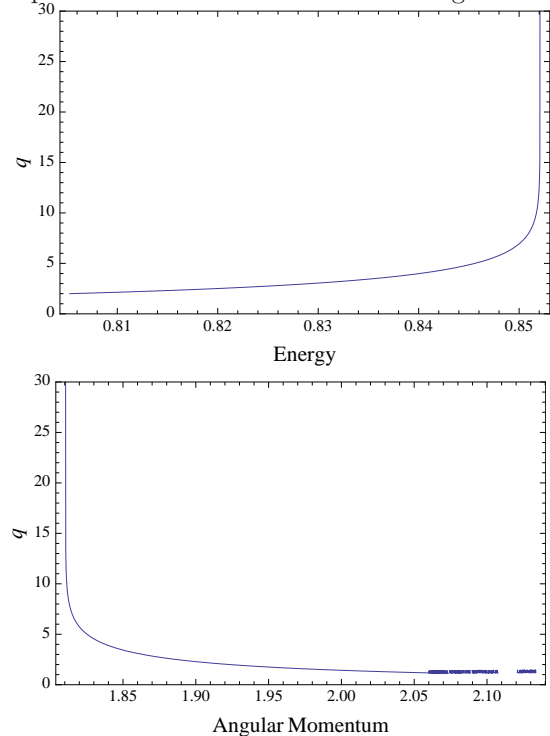


FIG. 5:  $a = 0.995$  Top:  $q$  versus  $E$  for  $L$  half way between the ibco and the isco,  $L = 1.81058$ . Bottom:  $q$  versus  $L$  for  $E = 0.852079$ .

black hole will cascade through a sequence of orbits, each of which looks like a precession of a low-leaf clover. As it inspirals into the black hole nucleus, it should leave an imprint of its transit through the periodic table in the gravitational radiation.

### \*Acknowledgements\*

I thank Glenna Clifton, Becky Grossman, Jamie Rollins and Pedro Ferreira for valuable conversations. I am especially grateful to Gabe Perez-Giz for his important contributions to this work. JL gratefully acknowledges financial support from an NSF grant AST-0908365.

[1] S. Chandrasekhar, *The Mathematical Theory of Black Holes*, Oxford: Clarendon Press, 1983.  
 [2] J. Levin and G. Perez-Giz, Phys. Rev. D **77**, 103005 (2008).

[3] K. Glampedakis and D. Kennefick, Phys. Rev. D **66**, 044002 (2002).  
 [4] B. Carter, Phys. Rev. **174**, 1559 (1968).  
 [5] S. Drasco and S. A. Hughes, Phys. Rev. D **69**, 044015

- (2004).
- [6] S. Drasco, E. Flanagan, and S. A. Hughes, *Class. Quant. Grav.* **22**, 801 (2005).
- [7] S. Drasco and S. Hughes, *Phys. Rev. D* **73**, 024027 (2006).
- [8] T. Hinderer and E. E. Flanagan, (2008).
- [9] S. Drasco, <http://www.tapir.caltech.edu/sdrasco/animations>, 2009.